



Contents lists available at ScienceDirect

International Communications in Heat and Mass Transfer

journal homepage: www.elsevier.com/locate/ichmt

Laminar heat transfer in a porous channel simulated with a two-energy equation model[☆]

Marcelo B. Saito, Marcelo J.S. de Lemos^{*}

Departamento de Energia – IEME, Instituto Tecnológico de Aeronáutica – ITA, 12228-900, São José dos Campos, SP, Brazil

ARTICLE INFO

Available online 12 August 2009

Keywords:

Two-energy equation
Porous media
Heat transfer coefficient

ABSTRACT

Laminar heat transfer in a porous channel is numerically simulated with a two-energy equation model for conduction and convection. Macroscopic equations for continuity, momentum and energy transport for the fluid and solid phases are presented. The numerical methodology employed is based on the control volume approach with a boundary-fitted non-orthogonal coordinate system. Fully developed forced convection in a porous channel bounded by parallel plates is considered. Solutions for Nusselt numbers along the channel are presented for laminar flows. Results simulate the effects Reynolds number Re , porosity, particle size and solid-to-fluid thermal conductivity ratio on Nusselt number, Nu , which is defined for both the solid and fluid phases. High Re , low porosities, low particle diameters and low thermal conductivity ratios promote thermal equilibrium between phases leading to higher values of Nu .

© 2009 Elsevier Ltd. All rights reserved.

1. Introduction

The assumption of local thermal equilibrium when analyzing heat transport in porous media requires several constraints which have been investigated in the literature [1–5]. For example, this condition is no longer valid when the particles or pores are not small enough, when the thermal properties differ widely, or when convective transport is not important. Furthermore, when there is a significant heat generation in any of the phases, the system will depart rapidly from the local thermal equilibrium state [6]. For such extreme conditions, the one-energy equation or one-temperature model is inadequate to correctly describe both the transients associated with the quench front penetrating the hot dry porous layer and regions where dry out occurs. When the assumption of local thermal equilibrium fails to be valid, one possible solution is to develop separate transport equations for each phase [7–9]. This leads to mathematical models that are referred to as thermal non-equilibrium models, which consider distinct energy equations for each phase. However, analyses of heat transfer in porous media based on two-equation models are more complex because they require information on interstitial heat transfer between phases as well as the interfacial surface area. Due to such requirement, investigators have worked on how to obtain the interfacial heat transfer coefficient. Examples of such efforts are found in the work of Wakao et al. [10], who obtained a heuristic correlation for closely packed bed and compared their results with experimental data. Also found in the literature is a

numerical correlation for the interfacial convective heat transfer coefficient, which was proposed by Kuwahara et al. [11] for laminar flow and was based on porosity dependency.

In previously published articles, a mathematical model for predicting turbulent flow in porous media has been presented [12], including buoyant flows [13,14] as well as channel flows through porous inserts [15], perforated baffles [16] and across macroscopic interfaces [17]. In all of the above, the so-called one-energy equation model was used, which invoked the local thermal equilibrium between the working fluid and solid matrix. Later, Saito and de Lemos [18] presented simulations for laminar flows thorough the void space of rods, which were arranged in arrays and simulated a repetitive unit cell in a model of a porous medium. In a following article [19], a proposition of a correlation for the interfacial heat transfer coefficient for turbulent flow in a packed bed was presented. Results in [18,19] contributed to the development of a macroscopic model for non-equilibrium heat transfer in porous media, but no results for macroscopic flow were presented.

The purpose of this contribution is to combine the flow [12] and thermal non-equilibrium [19] models for porous media and predict macroscopic forced convection in a porous channel bounded by parallel plates.

2. Macroscopic transport

2.1. Flow equations

Macroscopic equations obtained after volume integration over a Representative Elementary Volume (REV) are given as [20,21],

$$\text{Continuity : } \nabla \cdot \mathbf{u}_D = 0. \quad (1)$$

[☆] Communicated by W.J. Minkowycz.

^{*} Corresponding author.

E-mail address: delemos@ita.br (M.J.S. de Lemos).

Nomenclature

Latin characters

A_i	interface area between fluid and solid phases
c_F	Forchheimer coefficient
c_p	fluid specific heat
D	particle diameter
Da	Darcy number, $Da = K/H^2$
h_i	interfacial heat transfer coefficient
\mathbf{I}	unit tensor
K	permeability
k_f	fluid thermal conductivity
k_s	solid thermal conductivity
\mathbf{K}_{disp}	dispersion tensor
$\mathbf{K}_{f,s}$	thermal conductivity tensor for fluid phase.
$\mathbf{K}_{s,f}$	thermal conductivity tensor for solid phase.
p	pressure
Pr	$Pr = \nu / \alpha$, Prandtl number
Re_D	Reynolds number based on D and superficial velocity \mathbf{u}_D
T	temperature
T_{ms}	average temperature of solid phase
T_{mf}	average temperature of fluid phase
u_B	bulk velocity
\mathbf{u}	local velocity
\mathbf{u}_D	Darcy or superficial velocity (volume average of \mathbf{u})
x, y	Cartesian coordinates, m
X, Y	non-dimensional coordinates, x/H and y/H

Greek characters

α	fluid thermal diffusivity
ΔV	representative elementary volume
ΔV_f	fluid volume inside ΔV
μ	fluid dynamic viscosity
ν	fluid kinematic viscosity
ρ	fluid density
ϕ	$\phi = \Delta V_f / \Delta V$, porosity

Subscripts

w	wall
s	solid phase
f	fluid phase

$$\text{Momentum} : \rho \left[\frac{\partial \mathbf{u}_D}{\partial t} + \nabla \cdot \left(\frac{\mathbf{u}_D \mathbf{u}_D}{\phi} \right) \right] = -\nabla(\phi \langle \bar{p} \rangle^i) + \mu \nabla^2 \mathbf{u}_D - \left[\frac{\mu \phi}{K} \mathbf{u}_D + \frac{c_F \phi \rho |\mathbf{u}_D| \mathbf{u}_D}{\sqrt{K}} \right], \quad (2)$$

where the last two terms in Eq. (2) represent the Darcy and Forchheimer contributions. The symbol K is the porous medium permeability, c_F is the form drag or Forchheimer coefficient, $\langle \bar{p} \rangle^i$ is the intrinsic average pressure of the fluid and ϕ is the porosity of the porous medium. In this work, the permeability is taken as a function of the particle diameter D as [22],

$$K = \frac{\phi^3 D^2}{144(1-\phi)^2}. \quad (3)$$

2.2. Energy equations

A two-energy equation model for convection and conduction in porous media, considering a heat transfer coefficient between the fluid and the solid phases, is given by the following equation set:

$$\left(\rho c_p \right)_f \left[\frac{\partial \phi \langle T_f \rangle^i}{\partial t} + \nabla \cdot \left\{ \phi \left(\mathbf{u}^i \langle T_f \rangle^i + \langle \mathbf{u}^i T_f \rangle^i \right) \right\} \right] = \nabla \cdot \left[k_f \nabla \left(\phi \langle T_f \rangle^i \right) \right] + \frac{1}{\Delta V} \int_{A_i} \mathbf{n}_i \cdot k_f \nabla T_f dA \quad (4)$$

$$\left(\rho c_p \right)_s \left\{ \frac{\partial (1-\phi) \langle T_s \rangle^i}{\partial t} \right\} = \nabla \cdot \left\{ k_s \nabla \left[(1-\phi) \langle T_s \rangle^i \right] \right\} - \frac{1}{\Delta V} \int_{A_i} \mathbf{n}_i \cdot k_s \nabla T_s dA \quad (5)$$

where, $\langle T_s \rangle^i$ and $\langle T_f \rangle^i$ denote the intrinsic average temperature of solid and fluid phases, respectively, A_i is the interfacial area within the REV. The convective transport is described in the second term on the right hand side of Eq. (4) (see Rocamora and de Lemos [23] for details).

2.2.1. Interfacial heat transfer

In Eqs. (4) and (5) the heat transferred between the two phases can be modeled by means of a film coefficient h_i such that,

$$h_i a_i \left(\langle T_s \rangle^i - \langle T_f \rangle^i \right) = \frac{1}{\Delta V} \int_{A_i} \mathbf{n}_i \cdot k_f \nabla T_f dA = \frac{1}{\Delta V} \int_{A_i} \mathbf{n}_i \cdot k_s \nabla T_s dA \quad (6)$$

where, $a_i = A_i / \Delta V$ is the interfacial area per unit volume. In porous media, the high values of a_i make them attractive for transferring thermal energy via conduction through the solid followed by convection to a fluid stream.

As mentioned earlier, Wakao et al. [10] obtained a correlation for closely packed bed of particle diameter D and compared their results with experimental data. This correlation for the interfacial heat transfer coefficient is given by,

$$\frac{h_i D}{k_f} = 2 + 1.1 Re_D^{0.6} Pr^{1/3}. \quad (7)$$

Further, a numerical correlation for the interfacial convective heat transfer coefficient was proposed by Kuwahara et al. [11] for laminar flow as,

$$\frac{h_i D}{k_f} = \left(1 + \frac{4(1-\phi)}{\phi} \right) + \frac{1}{2} (1-\phi)^{1/2} Re_D Pr^{1/3}, \quad \text{valid for } 0.2 < \phi < 0.9. \quad (8)$$

Eq. (8) is based on porosity dependency and is valid for packed beds of particle diameter D . In addition, Saito and de Lemos [18] numerically calculated the interfacial heat transfer coefficient h_i for laminar flow through an infinite rod array. In their physical model, the porous medium was considered to be formed by a large number of regularly arranged solid square rods. This same methodology was applied by Saito and de Lemos [19], who proposed a correlation for h_i for turbulent flow as,

$$\frac{h_i D}{k_f} = 0.08 \left(\frac{Re_D}{\phi} \right)^{0.8} Pr^{1/3}; \quad \text{for } 1.0 \times 10^4 < \frac{Re_D}{\phi} < 2.0 \times 10^7, \quad \text{valid for } 0.2 < \phi < 0.9. \quad (9)$$

2.2.2. Thermal dispersion

In order to apply Eq. (4) to obtain the fluid temperature field in porous media, the thermal dispersion term, 3rd term on the r.h.s of

Eq. (4), needs to be modeled as a function of the intrinsically averaged temperature $\langle T_f \rangle^i$. To accomplish this, a gradient type diffusion model is applied, such that:

$$-(\rho c_p)_f (\phi \langle \mathbf{u}^i T_f \rangle^i) = K_{disp} \cdot \nabla \langle T_f \rangle^i \quad (10)$$

Following Kuwahara and Nakayama [24] and Nakayama and Kuwahara [25], expressions for the components of thermal dispersion tensor can be used for $Pe_D \geq 10$ as,

$$\frac{(K_{dis})_{xx}}{k_f} = 2.1 \frac{Pe_D}{(1-\phi)^{0.1}}, \text{ for longitudinal dispersion,} \quad (11)$$

$$\frac{(K_{dis})_{yy}}{k_f} = 0.052(1-\phi)^{0.5} Pe_D, \text{ for transverse dispersion,} \quad (12)$$

where $(K_{disp})_{xx}$ and $(K_{disp})_{yy}$ are the transverse and longitudinal components of \mathbf{K}_{disp} , respectively.

2.2.3. Two-energy equation modeling

Using the models shown above for thermal dispersion and interfacial heat transfer, Eqs. (4) and (5) can be rewritten as:

$$\left\{ (\rho c_p)_f \phi \right\} \frac{\partial \langle T_f \rangle^i}{\partial t} + (\rho c_p)_f \nabla \cdot (\mathbf{u}_D \langle T_f \rangle^i) = \nabla \cdot \left\{ \mathbf{K}_{eff,f} \cdot \nabla \langle T_f \rangle^i \right\} + h_i a_i (\langle T_s \rangle^i - \langle T_f \rangle^i), \quad (13)$$

$$\left\{ (1-\phi)(\rho c_p)_s \right\} \frac{\partial \langle T_s \rangle^i}{\partial t} = \nabla \cdot \left\{ \mathbf{K}_{eff,s} \cdot \nabla \langle T_s \rangle^i \right\} - h_i a_i (\langle T_s \rangle^i - \langle T_f \rangle^i), \quad (14)$$

where, $\mathbf{K}_{eff,f}$ and $\mathbf{K}_{eff,s}$ are the effective conductivity tensor for fluid and solid, respectively, given by:

$$\mathbf{K}_{eff,f} = [\phi k_f] \mathbf{I} + \mathbf{K}_{disp}, \quad (15)$$

$$\mathbf{K}_{eff,s} = [(1-\phi)k_s] \mathbf{I}, \quad (16)$$

and \mathbf{I} is the unit tensor.

3. Non-dimensional parameters

The longitudinal Nusselt number is calculated for both the fluid and solid phases and is defined as [26],

$$\text{Fluid phase Nusselt number : } Nu_f = - \frac{2H}{T_w - T_{mf}} \left(\frac{\partial \langle T_f \rangle^i}{\partial y} \right), \quad (17)$$

$$\text{Solid phase Nusselt number : } Nu_s = - \frac{2H}{T_w - T_{ms}} \left(\frac{\partial \langle T_s \rangle^i}{\partial y} \right), \quad (18)$$

where T_{mf} and T_{ms} are the average temperature of the fluid and the solid phase, respectively, and are defined as follows;

$$T_{mf} = \frac{\int u T_f dy}{u_B H}, u_B = \frac{\int u dy}{H}, T_{ms} = \frac{\int T_s dy}{H}. \quad (19)$$

4. Numerical method and boundary conditions

The problem under investigation is a flow through a channel completely filled with a porous medium, as shown in Fig. 1. Boundary conditions for laminar flows in porous media are similar to the clear

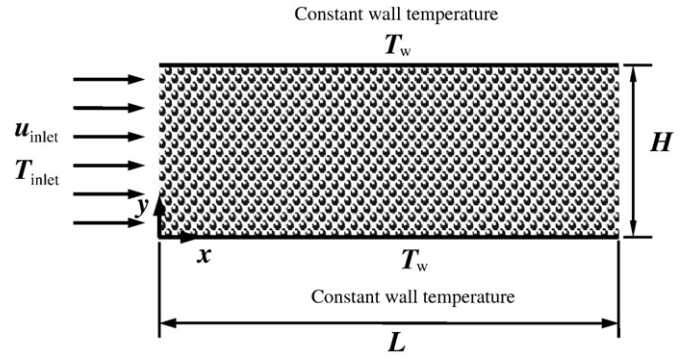


Fig. 1. Geometry under investigation and coordinate system.

channel flow. The numerical method used to discretize the flow and energy equations was the Control Volume approach. The SIMPLE method of Patankar [27] was applied for relaxing the systems of

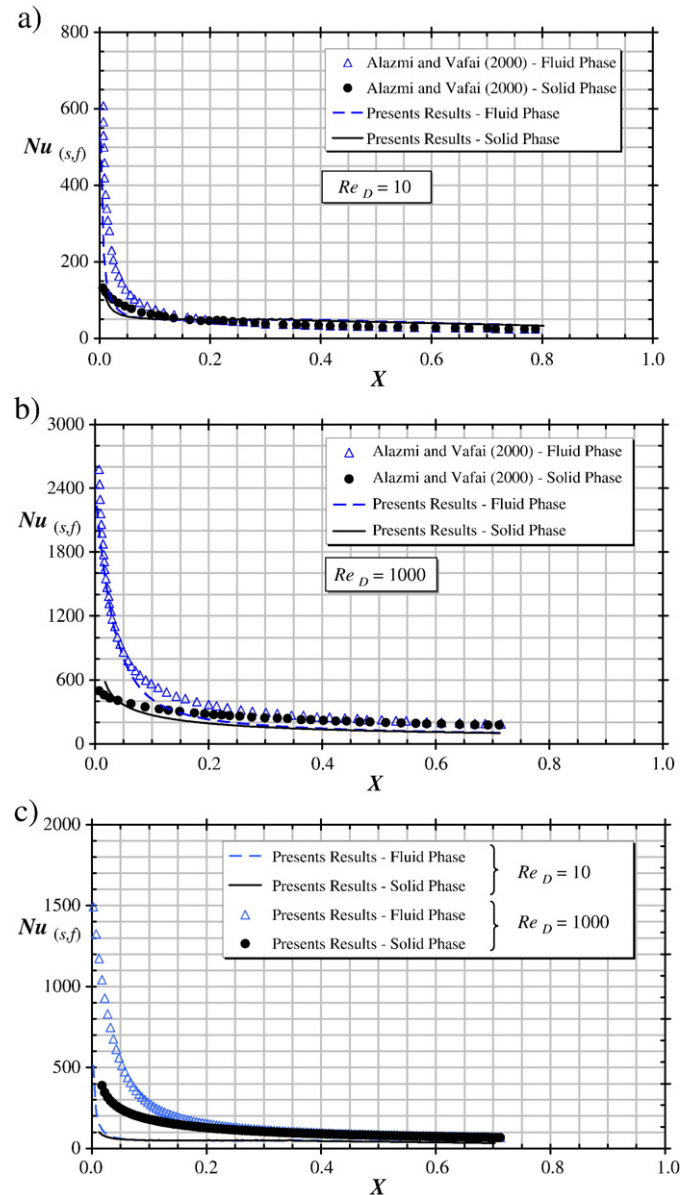


Fig. 2. Effect of Re on longitudinal Nusselt number. $Da = 10^{-4}$; $\phi = 0.6$; $D/H = 5.2 \times 10^{-2}$; $k_s/k_f = 25$; a) $Re_D = 10$, b) $Re_D = 1000$, c) both Re , present results.

algebraic equations. Convergence was monitored in terms of the normalized residue, which was set to be lower than 10^{-9} .

Boundary conditions are given by:

$$\text{On the solid walls : } \langle \mathbf{u} \rangle^i = 0, \langle T_s \rangle^i = \langle T_f \rangle^i = T_w, \quad (20)$$

$$\text{On the entrance : } \mathbf{u}_D = \mathbf{u}_{\text{inlet}}, \langle T_s \rangle^i = \langle T_f \rangle^i = T_{\text{inlet}}. \quad (21)$$

5. Results and discussion

The effect of the Reynolds number is shown in Fig. 2 compared with similar computations by Alazmi and Vafai [26]. The Reynolds number is found to have a substantial effect on the development length for Nu along the channel. Fig. 2c seems to indicate that for lower Reynolds number, the thermal equilibrium condition is achieved faster than for higher Reynolds number cases. Both solid and fluid temperatures reach an equilibrium value along X , decreasing the Nu difference along the channel.

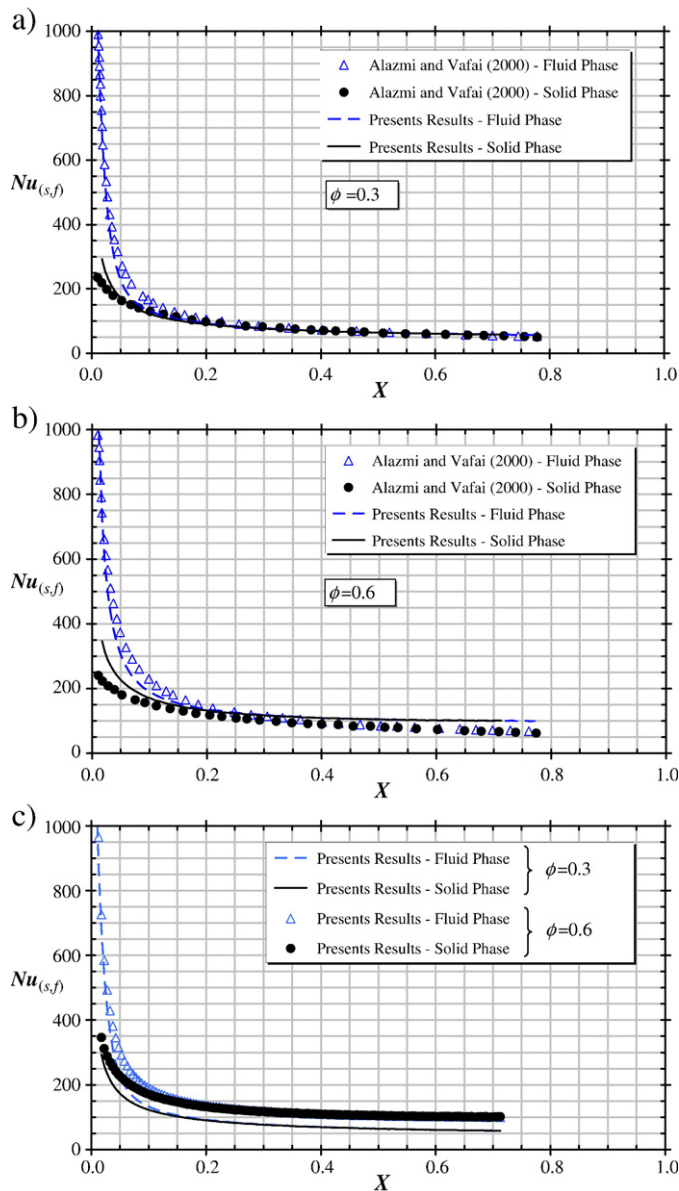


Fig. 3. Effect of porosity on longitudinal Nusselt number, $Re_D = 100$, $D/H = 5.2 \times 10^{-2}$, $k_s/k_f = 25$: a) $\phi = 0.3$, b) $\phi = 0.6$, c) both porosities, present results.

Fig. 3 shows the effect of porosity on Nusselt for both phases. It is observed from Fig. 3a and b) that the lower the porosity, the smaller the differences between the present results and those by Alazmi and Vafai [26]. For thermally developed flow and low porosity, both sets of results are closer to each other. Also, the higher the porosity, the higher the Nu number. High porosity condition means a lower interfacial area a_i , reducing the exchange of energy between phases, leading ultimately to higher values of Nu . Fig. 3c presents similar results in each phase for the entrance region of parallel plates.

The particle diameter, D , is directly related to the interfacial area a_i and appears in the expressions for h_i . Low values for D are associated with high interfacial areas and high interfacial film coefficients. As such, for the same porosity smaller particle diameters promote thermal equilibrium between phases by increasing the area of contact between the solid and the fluid. On the other hand, larger particle diameters tend to impair thermal equilibrium between phases, as seen in Fig. 4a,b. Fig. 4c shows the difference between each phase for

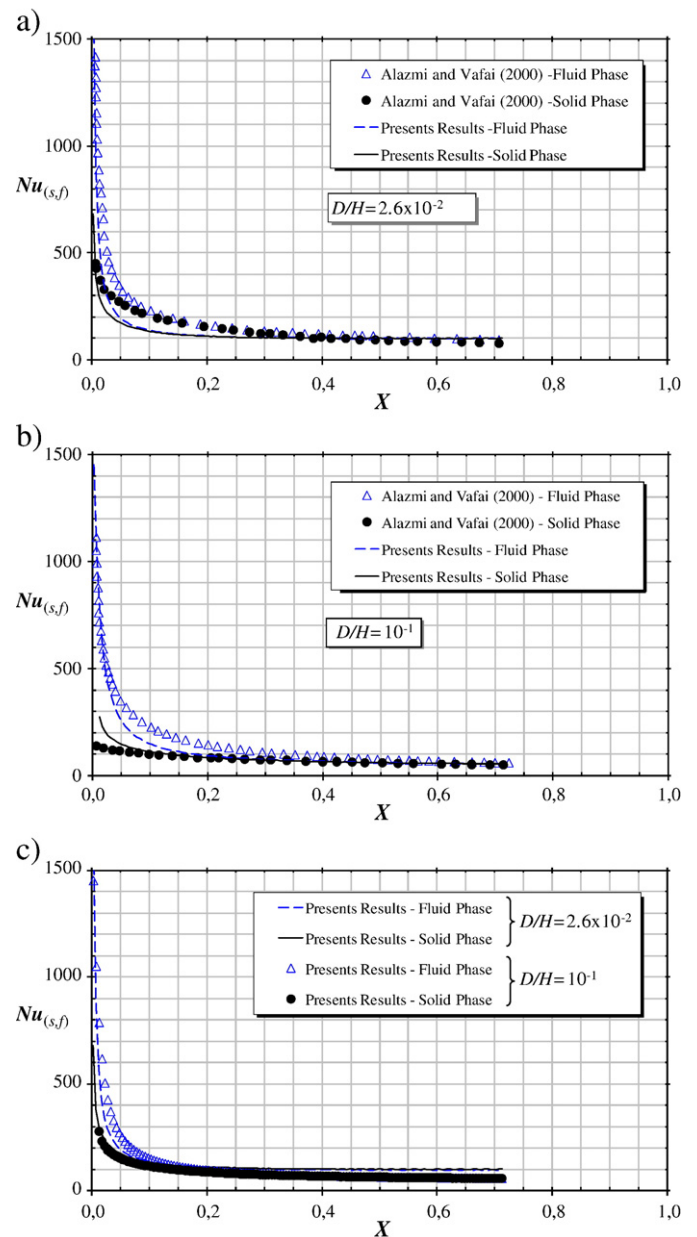


Fig. 4. Effect of D on longitudinal Nusselt number. $Da = 10^{-4}$, $Re_D = 100$; $\phi = 0.6$; $k_s/k_f = 25$: a) $D/H = 2.6 \times 10^{-2}$, b) $D/H = 10^{-1}$, c) both D/H ratios, present results.

distinct values of D and shows that thermal equilibrium is reached faster for smaller particle diameters. Also shown is that the larger particle diameters impair thermal equilibrium, affecting temperature distributions and leading to lower Nu numbers for both phases.

Fig. 5 shows the effect of thermal conductivity ratio on Nu . As seen in Fig. 5a and b, a lower conductivity ratio enhances thermal equilibrium by reducing temperature differences between phases. Fig. 5c presents a comparison of Nusselt numbers indicating that for a high conductivity ratio, impairment on the exchange of energy between phases affects local temperature values, ultimately reducing corresponding Nusselt numbers.

Finally, Fig. 6 shows a comparison of present results and those by Wakao et al. [10] and Kuwahara et al. [11] correlations in addition to results by Alazmi and Vafai [26]. It is clearly seen from Fig. 6 that a reasonable agreement is found between the predictions, except for the Kuwahara correlation [11] for the fluid phase Nusselt number, which is slightly higher. This discrepancy could be explained due to

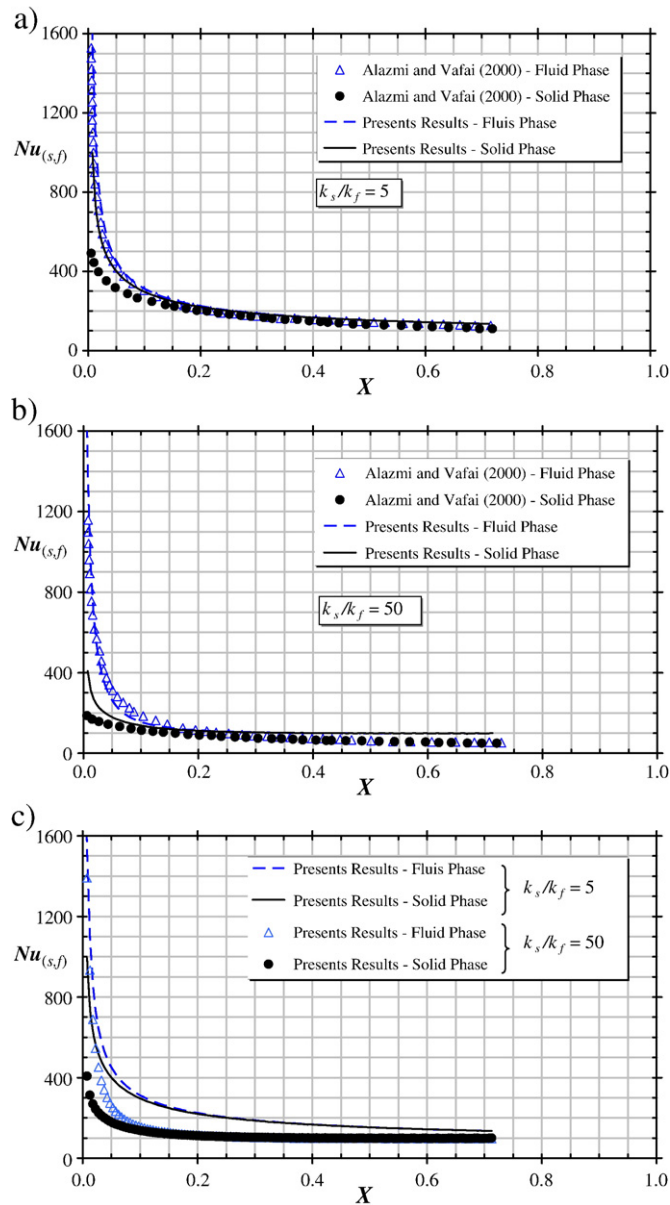


Fig. 5. Effect of solid-to-fluid thermal conductivity ratio on longitudinal Nusselt number. $Da = 10^{-4}$; $Re_D = 100$; $\phi = 0.6$; $D/H = 5.2 \times 10^{-2}$; a) $k_s/k_f = 5$, b) $k_s/k_f = 50$, c.) Both k_s/k_f ratios, present results.

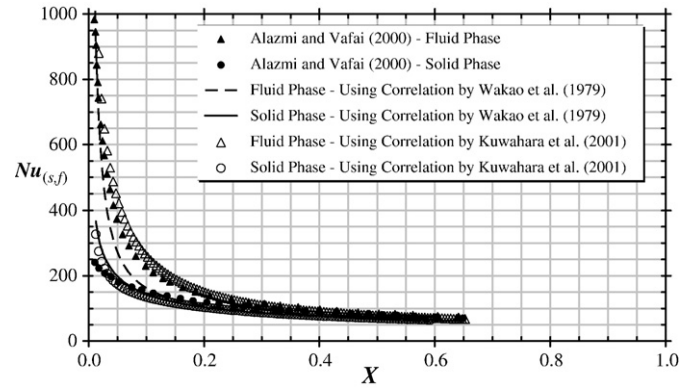


Fig. 6. Comparison between present results with various correlations and Alazmi and Vafai [26] results. $Da = 10^{-4}$; $Re_D = 100$; $\phi = 0.6$; $D/H = 5.2 \times 10^{-2}$; $k_s/k_f = 25$.

the fact that predictions by Alazmi and Vafai [26] were obtained with Wakao correlation [10], which is calculated considering a_i based on circular rods instead of square rods.

6. Concluding remarks

Fully developed forced convection in a porous channel bounded by parallel plates based on a two-energy equation model is analyzed. Details are presented for determining Nusselt numbers for laminar flows in a porous medium. Results simulate the effects of Re , ϕ , D and k_s/k_f on Nu . High Re , low porosities, low particle diameters and low thermal conductivity ratios promote thermal equilibrium between phases, eventually leading to higher values of Nu for both the fluid and the solid. Further work will be carried out in order to simulate fully turbulent flow and heat transfer in a porous medium with the macroscopic two-energy equation model.

Acknowledgments

The authors are thankful to CNPq and FAPESP, Brazil, for their invaluable financial support during the course of this research.

References

- [1] T.E.W. Schumann, Heat transfer: liquid flowing through a porous prism, J. Franklin Inst. 208 (1929) 405–416.
- [2] S. Whitaker, Improved constraints for the principle of local thermal equilibrium, Ind. Eng. Chem. Res. 30 (1991) 983–997.
- [3] M. Quintard, S. Whitaker, Local thermal equilibrium for transient heat conduction: theory and comparison with numerical experiments, Int. J. Heat Mass Transfer 38 (1995) 2779–2796.
- [4] M. Quintard, S. Whitaker, One- and two-equation models for transient diffusion processes in two-phase systems, Advances in Heat Transfer, 23, Academic Press, New York, 1993, pp. 369–464.
- [5] K. Vafai, M. Sozen, Analysis of energy and momentum transport for fluid flow through a porous bed, J. Heat Transfer 112 (1990) 690–699.
- [6] M. Kaviany, Principles of Heat Transfer in Porous Media, 2nd ed. Springer, New York, 1995.
- [7] M. Quintard, Modeling local non-equilibrium heat transfer in porous media, Proc. 11th Int. Heat Transfer Conf., Kyongyu, Korea, vol. 1, 1998, pp. 279–285.
- [8] D.B. Ingham, I. Pop, Transport Phenomena in Porous Media, Elsevier, Amsterdam, 1998, pp. 103–129.
- [9] M. Quintard, M. Kaviany, S. Whitaker, Two-medium treatment of heat transfer in porous media: numerical results for effective properties, Adv. Water Resour. 20 (1997) 77–94.
- [10] N. Wakao, S. Kaguei, T. Funazkri, Effect of fluid dispersion coefficients on particle-to-fluid heat transfer coefficients in packed bed, Chem. Eng. Sci. 34 (1979) 325–336.
- [11] F. Kuwahara, M. Shirota, A. Nakayama, A numerical study of interfacial convective heat transfer coefficient in two-energy equation model for convection in porous media, Int. J. Heat Mass Transfer 44 (2001) 1153–1159.
- [12] M.H.J. Pedras, M.J.S. de Lemos, On the definition of turbulent kinetic energy for flow in porous media, Int. Comm. Heat Mass Transfer 27 (2) (2000) 211–220.
- [13] E.J. Braga, M.J.S. de Lemos, Turbulent natural convection in a porous square cavity computed with a macroscopic k -epsilon model, Int. J. Heat Mass Transfer 47 (26) (2004) 5639–5650.

- [14] E.J. Braga, M.J.S. de Lemos, Heat transfer in enclosures having a fixed amount of solid material simulated with heterogeneous and homogeneous models, *Int. J. Heat Mass Transfer* 48 (23–24) (2005) 4748–4765.
- [15] M. Assato, M.J.H. Pedras, M.J.S. de Lemos, Numerical solution of turbulent channel flow past a backward-facing-step with a porous insert using linear and non-linear $k-\epsilon$ models, *J. Porous Media* 8 (1) (2005) 13–29.
- [16] N.B. Santos, M.J.S. de Lemos, Flow and heat transfer in a parallel-plate channel with porous and solid baffles, *Num. Heat Transf., A – Appl.* 49 (5) (2006) 471–494.
- [17] M.J.S. de Lemos, R.A. Silva, Turbulent flow over a layer of a highly permeable medium simulated with a diffusion-jump model for the interface, *Int. J. Heat Mass Transfer* 49 (3–4) (2006) 546–556.
- [18] M.B. Saito, M.J.S. de Lemos, Interfacial heat transfer coefficient for non-equilibrium convective transport in porous media, *Int. Comm. Heat Mass Transfer* 32 (5) (2005) 667–677.
- [19] M.B. Saito, M.J.S. de Lemos, A Correlation for interfacial heat transfer coefficient for turbulent flow over an array of square rods, *J. Heat Transfer* 128 (2006) 444–452.
- [20] W.G. Gray, P.C.Y. Lee, On the theorems for local volume averaging of multiphase system, *Int. J. Multiph. Flow* 3 (1977) 333–340.
- [21] J.C. Slattery, Flow of viscoelastic fluids through porous media, *AIChE J.* 13 (1967) 1066–1071.
- [22] S. Ergun, Fluid flow through packed columns, *Chem. Eng. Prog.* 48 (2) (1952) 89–94.
- [23] F.D. Rocamora Jr, M.J.S. de Lemos, Analysis of convective heat transfer of turbulent flow in saturated porous media, *Int. Comm. Heat Mass Transfer* 27 (6) (2000) 825–834.
- [24] F. Kuwahara, A. Nakayama, H. Koyama, A numerical study of thermal dispersion in porous media, *J. Heat Transfer* 118 (1996) 756–761.
- [25] A. Nakayama, F. Kuwahara, A macroscopic turbulence model for flow in a porous medium, *J. Fluids Eng.* 121 (1999) 427–433.
- [26] B. Alazmi, K. Vafai, Analysis of variants within the porous media transport models, *J. Heat Transfer* 122 (2000) 303–326.
- [27] S.V. Patankar, *Numerical Heat Transfer and Fluid Flow*, Hemisphere, Washington, DC, 1980.